Photosynthesis Research **82:** 83–94, 2004.

Regular paper

Triplet excitation transfer between carotenoids in the LH2 complex from photosynthetic bacterium *Rhodopseudomonas palustris*

Juan Feng[1], Qian Wang[2], Yi-Shi Wu[1], Xi-Cheng Ai[1], Xu-Jia Zhang[2], You-Guo Huang[2], Xing-Kang Zhang[1]& Jian-Ping Zhang[1,*]

[1]*The State Key Laboratory for Structural Chemistry of Unstable and Stable Species, Institute of Chemistry, Chinese Academy of Sciences, 1st North Street, Haidian District, Beijing 100080, P. R. China;* [2]*The National Laboratory of BioMacromolecules, Institute of Biophysics, Chinese Academy of Sciences, Beijing 100101, P. R. China; *Author for correspondence (e-mail: jpzhang@mail.iccas.ac.cn; fax: +86-10-82616163)*

Received 1 February 2004; accepted in revised form 1 April 2004

Key words: bacteriochlorophyll, carotenoid, light-harvesting antenna complex, time-resolved spectroscopy, triplet excitation transfer

Abstract

We have studied, by means of sub-microsecond time-resolved absorption spectroscopy, the triplet-excited state dynamics of carotenoids (Cars) in the intermediate-light adapted LH2 complex (ML–LH2) from *Rhodopseudomonas palustris* containing Cars with different numbers of conjugated double bonds. Following pulsed photo-excitation at 590 nm at room temperature, rapid spectral equilibration was observed either as a red shift of the isosbestic wavelength on a time scale of 0.6–1.0 μs, or as a fast decay in the shorter-wavelength side of the $T_n \leftarrow T_1$ absorption of Cars with a time constant of 0.5–0.8 μs. Two major spectral components assignable to Cars with 11 and 12 conjugated double bonds were identified. The equilibration was not observed in the ML–LH2 at 77 K, or in the LH2 complex from *Rhodobacter sphaeroides* G1C containing a single type of Car. The unique spectral equilibration was ascribed to temperature-dependent triplet excitation transfer among different Car compositions. The results suggest that Cars of 11 and 12 conjugated bonds, both in close proximity of BChls, may coexist in an α,β-subunit of the ML–LH2 complex.

Abbreviations: BChl – bacteriochlorophyll; Car – cartotenoid; LH2 – light-harvesting complex II; ML–LH2 – intermediate-light adapted LH2

Introduction

Carotenoid (Car) plays important physiological roles of light-harvesting and photoprotection in photosynthetic organisms (Frank and Cogdell 1993). For light-harvesting it absorbs light in the blue-green spectral region where bacteriochlorophyll (BChl) does weakly, and transfers the singlet electronic excitation to BChls (Koyama et al. 1996; Ritz et al. 2000). For photoprotection it quenches, via efficient BChl-to-Car energy transfer, triplet-excited state BChl (^{3}BChl*) before the formation of harmful singlet oxygen, or scavenges singlet oxygen directly (Cogdell et al. 2000). A common structural basis of the above physiological functions is the close proximity of Car and BChl molecules as found in a number of integral photosynthetic pigment-protein complexes by means of X-ray crystallography, e. g., bacterial reaction centers from *Rhodopseudomonas* (*Rps.*) *viridis* (Deisenhofer et al. 1985) and *Rhodobacter* (*Rb.*) *sphaeroides* (Allen et al. 1987; Ermler et al. 1994), and light-harvesting antenna complexes II (LH2) from *Rps. acidophila* (McDermott et al. 1995) and *Rhodospirillum* (*Rs.*) *molischianum* (Koepke et al. 1996). In the LH2 complex from *Rs. molischianum*, for an instance,

the closest edge-to-edge distance between lycopene and BChl molecules is ~3.4 Å, a distance facilitating the reaction of efficient BChl-to-Car triplet energy transfer (Damjanović et al. 1999).

Early laser flash photolysis studies on chromatophores, reaction centers and antenna complexes of photosynthetic bacteria had shown the formation of triplet-excited state Car (^{3}Car*) upon photoexcitation of either BChls or Cars (Monger et al. 1976, 1977; Rademaker et al. 1980; Cogdell et al. 1981; Kingma et al. 1985). These experiments and a later theoretical work (Nagae et al. 1993) had established the reaction of efficient BChl-to-Car triplet energy transfer with a timescale of ~10 ns which is governed by electron-exchange coupling [Dexter's theory (Dexter 1953)]. This mechanism has recently been reconfirmed by a theoretical analysis based on detailed crystallographic data available for the LH2 complex from *Rs. molischianum* (Damjanović et al. 1999) and, by a direct experimental demonstration on the LH2 from *Rb. sphaeroides* (Bittl et al. 2001). In addition, an unusual mechanism of ^{3}Car* formation proceeding on femtosecond and picosecond timescales in the light-harvesting complexes from *Rs. rubrum* was newly identified, and was suggested to be intra-molecular singlet fission of Car (Gradinaru et al. 2001).

Depending on the growth condition, the LH2 complex from *Rps. palustris* was categorized into three different 'spectral forms', i.e., the low-light form (LL) grown under a photon flux of ~100 lux, the intermediate-light form (ML) under ~1000 lux, and the high-light form (HL) under ~7000 lux (Tharia et al. 1999). These spectral forms are spectroscopically distinguishable in terms of the relative intensity between the absorption bands of B800 and B850 BChls in the near-infrared spectral region at 800 nm and 850 nm, respectively. The LH2 complexes from *Rps. palustris* are unique in the heterogeneous composition of Cars. Total of 5 Cars with different numbers of conjugated C=C bonds ($N_{C=C}$) were identified as lycopene (11), rhodopin (11), rhodovibrin (12), anhydrorhodovibrin (12) and spirilloxanthin (13), and the content of individual Cars as well as the molecular ratio of BChl:Car vary upon different spectral forms (Evans et al. 1990). Hartigan et al. have recently succeeded in isolating a novel LL–LH2 complex and obtained its electron density map at a 7.5-Å resolution, which clearly shows an 8-fold symmetric aggregate structure of α,β-subunits with unique apoprotein expression (Hartigan et al. 2002). The authors also proposed a model of geometric arrangement of BChls based on the electron density map and on an effort to fit the near-infrared absorption and circular dichroism data. Regarding the arrangement of Car molecules in the LH2 complexes, however, no detailed structural information has been available.

The above peculiarities of the LH2 complexes from *Rps. palustris* are both interesting and challenging for spectroscopic studies on the singlet and the triplet energy-transfer reactions among BChl and Car molecules. We are interested in the triplet excited-state dynamics among the heterogeneous Car compositions, and the present paper reports the results of the ML–LH2 complex obtained by the use of sub-microsecond time-resolved absorption spectroscopy both at room temperature and at 77 K. Following pulsed photo-excitation of BChls, rapid spectral relaxation on a timescale of 0.6–1.0 μs in the $T_n \leftarrow T_1$ absorption of Cars was observed, which could be attributed to the equilibration dynamics of triplet excitation among different types of Cars, and was found to be temperature dependent. A total of 2 major spectral components assignable to the 2 groups of Cars with 11 and 12 conjugated double bonds were clearly identified with the help of a global analysis on the time-resolved data. The results are discussed in light of the number of Cars and their locations with reference to BChl cofactors in an α,β-subunit of the ML–LH2 complex from *Rps. palustris*.

Materials and methods

Isolation and purification of LH2 complexes

Cells of *Rps. palustris* were grown photoheterotrophically in Bose media (Bose 1963) at a light intensity of ~4000 lux at 28 °C for about 50 h. The intermediate-light adapted LH2 complex (ML–LH2) was isolated and purified basically following the method described by Evans et al. (1990) with certain modification. The cells harvested were sonicated at 4 °C (Cole parmer Ultrasonic homogenizer CPX 600) and digested by lysozyme (1 mg ml^{-1}) for an hour, and the pellets (mem-

branes) were precipitated by centrifugation at 150,000 × *g* for an hour at 4 °C and re-suspended in 20 mM Tris-HCl (pH 8.0) to give an absorption maximum of 50 cm^{-1} at 880 nm. The membranes were further solubilized with 1% (v/v) lauryldimethylamine *N*-oxide (LDAO) and centrifuged at 5000 × *g* for 10 min to remove the unsolubilized debris. The supernatant was then diluted with 20 mM Tris-HCl (pH 8.0) to bring the LDAO concentration to 0.3% (v/v) and layered onto a sucrose step gradients consisting of 0.3, 0.6 and 1.2 M sucrose in 20 mM Tris-HCl (pH 8.0) and 0.1% (v/v) LDAO. The gradients were centrifuged at 150,000 × *g* for 16 h at 4 °C and the protein band located between 0.3 and 0.6 M sucrose was collected and dialyzed against the buffer containing 20 mM Tris-HCl (pH 8.0) and 0.1% LDAO. The purity of the ML–LH2 complexes was >95% as estimated by the use of absorption spectrum and SDS-PAGE. Figure 1 shows the room-temperature absorption spectrum of the purified ML–LH2.

The LH2 complex from *Rb. sphaeroides* G1C was prepared following the procedures reported by Fujii et al. (1998).

Analysis of pigment compositions

The pigment extraction and the HPLC analysis of Car composition were carried out following the procedures and the HPLC conditions described by Qian et al. (2001). Briefly, the complete acetone/methanol (7 : 2, v/v) extract of pigments from the ML–LH2 suspension was further dissolved in petroleum ether. Saturated sodium chloride solution was then added to transfer the pigments into the petroleum–ether layer, and the procedure was repeated until the complete extraction of pigments. The pigment-containing epiphase was dried by the use of a rotary evaporator in the dark, and the extract was then dissolved in HPLC-grade acetone/benzene (1 : 40, v/v) that was used as the eluent for the subsequent HPLC analysis. The HPLC analysis was done with a silica gel column (Alltima silica, 5 μm, 25 × 0.46 cm; Alltech Associates) on a Hitachi system equipped with a photodiode array detector (Hitachi, L-7455). Cars were identified by their UV–visible spectra from 350 to 600 nm. The relative contents of all the Cars in the ML–LH2 complex were determined by integrating the elution amplitude, and by using the reported molar extinction coefficients of Cars at 480 nm in the same eluent (Qian et al. 2001). The results of HPLC analysis are presented in Table 1.

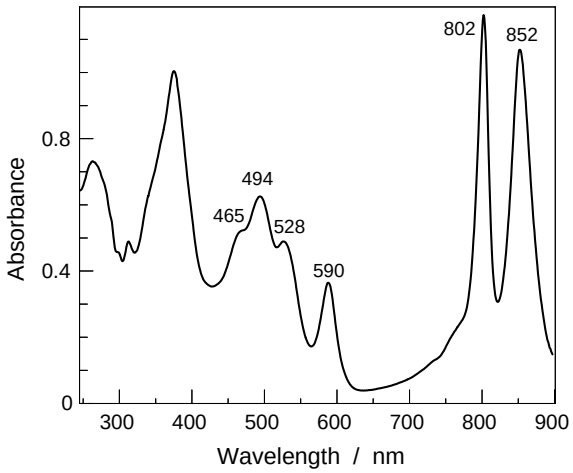

Figure 1. Room-temperature (295 K) absorption spectrum of the LH2 complex from *Rhodopseudomonas palustris* grown under an intermediate light level (ML) of ~4000 lux. Numerals indicate the peak wavelengths in nm.

The BChl-to-Car molecular ratio was determined from the UV–visible spectrum of the pigment extracts in the HPLC eluent. An average extinction coefficient of 138.1 mM^{-1} cm^{-1} at 480 nm was used for Cars, whereas that for BChl *a* was 85 mM^{-1} cm^{-1} at 772 nm. The latter coefficient was estimated by recording the absorbance of BChl *a* either in acetone/methanol [$\varepsilon_{772\ nm}$ = 76 mM^{-1} cm^{-1} (Clayton et al. 1966)] or in ethanol [$\varepsilon_{774\ nm}$ = 62 mM^{-1} cm^{-1} (Connolly et al. 1982)], drying and re-dissolving it with the same volume of eluent, and then calculating the coefficient with reference to the known extinction coefficients. The BChl-to-Car ratio thus obtained is 2.5 ± 0.2:1 as an average of four independent determinations on two different ML–LH2 preparations.

Sub-microsecond time-resolved spectroscopy

For the measurements at room temperature (295 K) oxygen was removed, when necessary, by adding 5 mM glucose, 0.1 mg ml^{-1} glucose oxidase and 0.05 mg ml^{-1} catalase to the LH2 preparation, a method that was used in spectroscopic studies on Photosystem II (Crystall et al. 1989). The sample cell was mounted on a translational stage to ensure that a fresh sample volume was exposed to each shot of pulsed excitation. For the

Table 1. Results of the HPLC analysis of Cars in the ML–LH2 complex from *Rhodopseudomonas palustris*

Retention time (min)	Carotenoid	Absorption wavelength [a] (nm)	Partial content [b] (%)	$N_{C=C}$
3.01	Lycopene	514.5	11.2 ± 1.0	11
3.96	Anhydrorhodovibrin	528.6	9.4 ± 0.2	12
5.68	Spirilloxanthin	538.9	12.4 ± 3.4	13
11.00	Rhodopin	514.3	32.2 ± 1.6	11
11.39	3,4-Didehydrorhodopin	528.7	26.4 ± 0.8	12
18.27	Rhodovibrin	528.6	2.8 ± 0.7	12
18.84	Monomethylated spirilloxanthin	538.9	5.6 ± 0.9	13

[a] The $1B_u^+(0) \leftarrow 1A_g^-(0)$ vibronic transition for Cars in the HPLC eluent of acetone/benzene (1:40, v/v).
[b] The extinction coefficients of rhodovibrin and spirilloxanthin reported by Qian et al. (2001) were used for 3,4-didehydrorhodopin and monomethylated spirilloxanthin, respectively, for the estimation of the partial contents.

measurements at cryogenic temperature (77 K), 60% glycerol (v/v) was added to the suspension, and the mixture was frozen rapidly by the use of a cryostat (ST-100, Lauis Research Co., Inc.) to form a glassy block of optical quality. The optical path lengths are 5 and 2.5 mm for the room-temperature and the 77-K measurements, respectively. The optical density at the excitation wavelength of 590 nm was adjusted to 0.3–0.4.

The excitation laser pulses (~7 ns, 3 Hz) at the wavelength of 590 nm were obtained from a dye laser (TDL-51, Quantel International) pumped by the second harmonic wave from a Nd:YAG laser (571C, Quantel International). The excitation energy was attenuated to ~1.5 mJ at the sample cell. White light pulses from a xenon flash lamp (L7685, Hamamatsu Photonics) were used as the probe. After passing the excited volume of sample the probe light was sent to a polychromator equipped with a gated linear photodiode array detector (1420, EG&G; gate width 50 ns). An electric delay pulse generator (DG535, Stanford Research System) was used to regulate the delay time between the excitation and the gate pulses, the latter of which had been synchronized to the probe pulse. This apparatus allowed us to record transient spectra at selected delay times. Global curve fitting was made over a number of kinetics at selected wavelengths, in which a sum of exponentials convoluted to a Gaussian instrumental response function (full width at half maximum, 50 ns) was used as a model function. Computer programs for the data analysis were compiled based on Matlab 5.2 (Mathworks) and Mathcad Pro7 (MathSoft).

Results

Pigment compositions of the ML–LH2 complex

The HPLC analysis has revealed heterogeneous Car compositions (Table 1). Seven different types of Cars, lycopene, anhydrorhodovirin, spirilloxanthin, rhodopin, 3,4-didehydrorhodopin, rhodovibrin and an unknown Car that is likely monomethylated spirilloxanthin present in the ML–LH2 complex. The above assignments were based on Qian's work on *Rhodobium marinum* that was done under the same HPLC conditions as here (Qian et al. 2001), the electronic absorption spectra of the elution components, as well as the spirilloxanthin biosynthesis pathway described by Schmidt for *Rps. palustris* (Schmidt 1978). The Cars can be categorized into 3 groups having 11, 12 and 13 conjugated double bonds with the partial contents of 43.4%, 38.6% and 18%, respectively. These Car compositions deviate considerably from those reported for LL–LH2 and HL–LH2 complexes from *Rps. palustris* by Evans et al. (1990), where spirilloxanthin constitutes more than 50% of the overall Car in either of the complexes. The relative high content of the Cars having 11 conjugated double bonds is also evidenced by the shorter peak wavelengths of the vibronic bands in the present study (Figure 1) compared to those in Evans et al. (1990), as well as by the clearer vibronic structures observed in the present study. The BChl-to-Car molecular ratio of 2.5 ± 0.2:1 implies that 1.2 ± 0.1 Car molecules associate with an α,β-subunit given the number of

BChls in it is 3 as in the cases of *Rps. acidophila* and *Rs. molischianum*. In view of the light-level dependent apoprotein expression of the LH2 complex for *Rps. palustris* (Tharia et al. 1999), Hartigan and co-worker's structure of LL–LH2 (Hartigan et al. 2002) may not be the same as the ML–LH2 complex in the present study. Nevertheless, if we take the number of BChls per α,β-subunit as 4 as suggested by Hartigan et al. (2002), the number of Car molecules can be 1.6 ± 0.1.

Dynamics of spectral equilibration

With the pulsed excitation at 590 nm, which corresponds to the Q_x absorption band of BChls, we recorded sub-microsecond time-resolved absorption spectra for the ML–LH2 of *Rps. palustris* at room temperature under both aerobic and anaerobic conditions, as well as those at 77 K, and the results are presented in Figures 2a–c. For comparison we also measured, at room temperature, the time-resolved spectra for the LH2 complex from *Rb. sphaeroides* G1C containing mainly all-*trans*-neurosporene ($N_{C=C} = 9$), and the results are shown in Figure 2d.

In all the sets of time-resolved spectra, bleaching of ground-state absorption appear to the shorter-wavelength side as negative signals immediately following the pulsed excitation (0.0 μs). They are accompanied by positive $T_n \leftarrow T_1$ absorption to the longer-wavelength side peaked at ~560 nm (Figures 2a, b) and ~566 nm (Figure 2c) under physiological and cryogenic temperatures, respectively, for the ML–LH2 of *Rps. palustris*, and at ~518 nm for the LH2 of *Rb. sphaeroides* G1C (Figure 2d). The triplet absorption spectra of the ML–LH2 are obviously much broader than those of the LH2, a fact that suggests the contribution from different Car compositions. In the 77-K measurement the triplet absorption band clearly splits into 2 peaks at ~550 and ~566 nm. The transient spectra reach a maximal ΔOD at the delay time of 0.05 μs under room temperature (Figures 2a, b), whereas a rising phase between 0.0 and 0.3 μs can be clearly identified in the 77-K case (Figure 2c). The absence of a rising phase at room temperature suggests that the formation of ^{3}Car* is faster than the present instrumental resolution (~50 ns). The temperature-dependent building-up phase of ^{3}Car* population observed in the present work is ascribed to the process of BChl-to-Car triplet energy transfer. It has been well established that ^{3}BChls* transfer the excitation energy efficiently to their adjacent Cars in bacterial antenna complexes. The timescale of energy transfer is temperature dependent, it is ~10 ns at room temperature, and slows down upon decreasing temperature with a pronounced relationship (Bittl et al. 2001).

We now examine the dynamics of spectral equilibration in the time-resolved absorption spectra at room temperature (Figures 2a, b). The dominant $T_n \leftarrow T_1$ absorption bands have a shoulder at ~545 nm in the delay time range of 0.0–0.3 μs, which appears at 0.0 μs with a higher intensity ratio with respect to the 560 nm main absorption, and decays completely within ~1.0 μs. This time-dependent change of transient spectra can be more clearly seen in Figure 3, where the transients are normalized after being smoothed by the use of a Gaussian kernel method. The rapid relaxation of the 545 nm shoulder is accompanied by a ~3 nm dynamic red shift of the isosbestic point around 500 nm (Figures 3a, b). In parallel with this shift the peak wavelength shifts to the red by ~2.5 nm. In contrast, spectral relaxation is not seen in the red edge of the $T_n \leftarrow T_1$ absorption bands. To characterize the dynamics of spectral relaxation we extracted the kinetics of time-dependent changes of the isosbestic wavelength as shown in the insets of Figures 3a and b. They could be fit to an exponential increase function in form of $1-exp(-t/\tau)$ with the time constant τ of 0.6 μs in the aerobic and 1.1 μs in the anaerobic cases. It is not surprising to find the dynamic spectral relaxation because the MH–LH2 contains different types of Cars and the lifetime of ^{3}Car* is conjugation-length dependent. However, the aforementioned unrelaxed red edges of the $T_n \leftarrow T_1$ bands, as well as the direction of the isosbestic point shift cannot be explained in terms of the general trend of the conjugation-length dependent lifetimes of triplet Cars and relative polyenes, i.e., the longer the conjugation-length, the shorter the lifetime (Truscott et al. 1973; Farhoosh et al. 1994). To the contrary, the 545-nm spectral component associated with a shorter-conjugated Car decays much faster than the 560 nm component with a longer-conjugated one. For the 77-K measurement, on the other hand, the isosbestic point of the time-resolved $T_n \leftarrow T_1$ spectra shows no appreciable time dependence (inset of Figure 3c). The different spectral dynamics

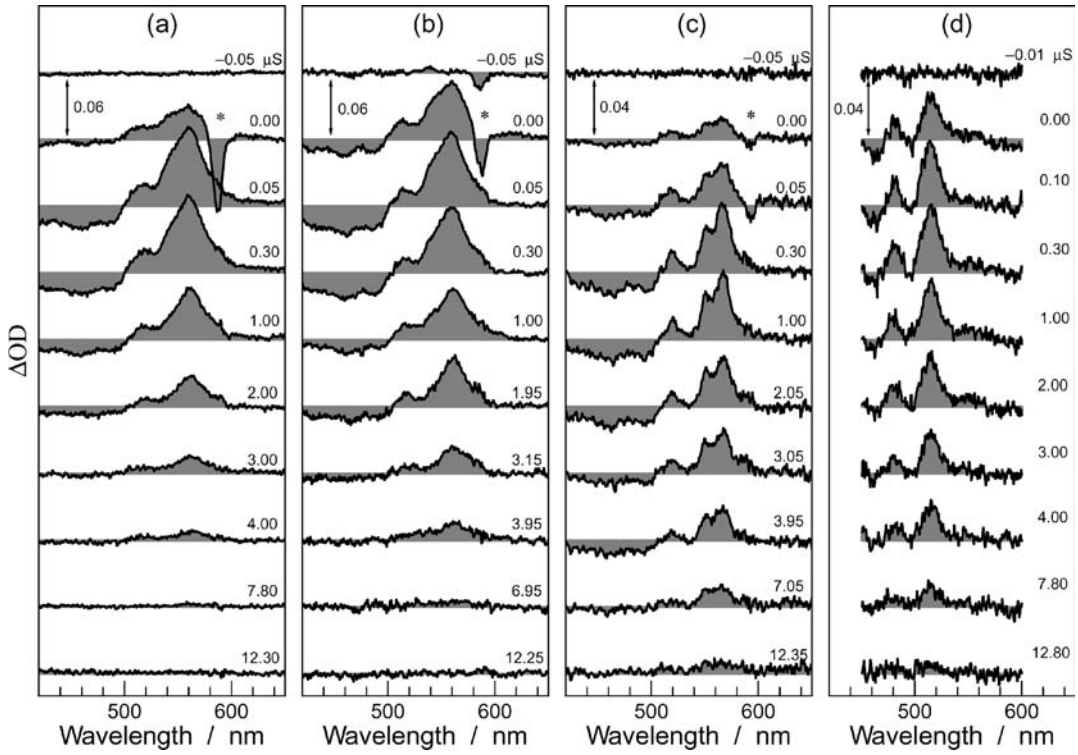

Figure 2. Time-resolved $T_n \leftarrow T_1$ absorption spectra of carotenoids in the ML–LH2 complex from *Rhodopseudomonas palustris* recorded following pulsed excitation at 590 nm at room temperature under (a) aerobic and (b) anaerobic conditions, and (c) those recorded at 77 K. (d) Time-resolved $T_n \leftarrow T_1$ absorption spectra of carotenoid (all-*trans*-neurosporene) in the LH2 complex from *Rhodobacter sphaeroides* G1C recorded at room temperature under the excitation wavelength of 355 nm. All the spectral curves (solid lines) are unsmoothed; Asterisks in Figures (a)–(c) indicate the laser interference. In each panel an arrow bar indicates the scale of absorbance change, and the delay times are given by the right-hand side numerals.

observed under physiological and cryogenic temperatures for the ML–LH2 from *Rps. palustris* is to be interpreted as the temperature-dependent reaction of triplet excitation transfer among different Car compositions. As a supporting evidence, the LH2 complex of *Rb. sphaeroides* G1C exhibits no spectral relaxation on either the red or the blue side of the $T_n \leftarrow T_1$ band (Figure 3d).

Identification and assignment of the transient spectral components

The above results have demonstrated, for the ML-LH2 from *Rps. palustris* at room temperature, the rapid spectral equilibration with a characteristic time constant of ~1 μs in the blue side of the main $T_n \leftarrow T_1$ bands. To extract the triplet-excited state dynamics of an individual Car from a set of time-resolved spectra, we carried out general-purpose global curve fitting over 28 representative wavelengths from 460 to 605 nm. The room-temperature data could be well accounted for by a summation of two exponential decays, whereas the 77-K data required an additional exponential component describing the rising phase in the set of original transients (Figure 2c, 0.0–0.3 μs). The decay associated difference spectra (DADS) and the corresponding time constants thus obtained are depicted in Figures 4a–c. At the top of panels a–c, the summation of DADS components 1 to 2 are shown (Sum). For all the three cases, the Sum spectra faithfully reflect the key features of the time-resolved spectra in the initial phase (e.g., those at 0.03 μs), a fact which proves a satisfactory fit. For comparison, global fitting was also applied to the time-resolved data of the LH2 from *Rb. sphaeroides* G1C. A 2-exponential decay function could fit the 28 kinetics curves nicely, and Figure 4d depicts the resulted DADS components and associated time constants. Figure 5 illustrates the calculated fitting curves along with the experimental data points at representative probe wave-

lengths for the ML–LH2 complexes, in which the rising phase with a time constant of 0.16 ± 0.05 μs is clearly seen in the 566 nm trace for the 77-K case.

At room temperature component-1 in Figure 4a and b contributes ~30% in amplitude to the Sum spectra as measured at its peak wavelength of 545 nm. This component can be ascribed to the $T_n \leftarrow T_1$ absorption by the group of Cars having 11 conjugated double bonds including lycopene and rhodopin. As the supporting evidence to this assignment, for spheroidene ($N_{C=C} = 10$) in the LH2 complex from *Rb. sphaeroides* 2. 4. 1, its $T_n \leftarrow T_1$ transition shifts about 7 nm to the red at 10 K [~537 nm (Angerhofer et al. 1995)] compared to the transition at room temperature [~530 nm (Monger et al. 1976)]. It was reported that Cars consisting of 11 conjugated double bonds in the LH2 complexes from *Rps. palustris* and *Rps. acidophila* have their $T_n \leftarrow T_1$ transition energies at ~550 nm at 10 K (Angerhofer et al. 1995; Bittl et al. 2001). Compared to the present result at room temperature, a ~5-nm red shift of $T_n \leftarrow T_1$ transition energy seems reasonable for Cars of $N_{C=C} = 11$ in the ML–LH2 complex. This type of red shift may originate from the increase in the solvent density upon decreasing the temperature, which results in a higher optical refractive index and hence higher solvent polarizability. The DADS of component-1 is coupled to a negative spectral section peaked at ~560 nm and ~585 nm. The 560 nm negative feature implies an intrinsic

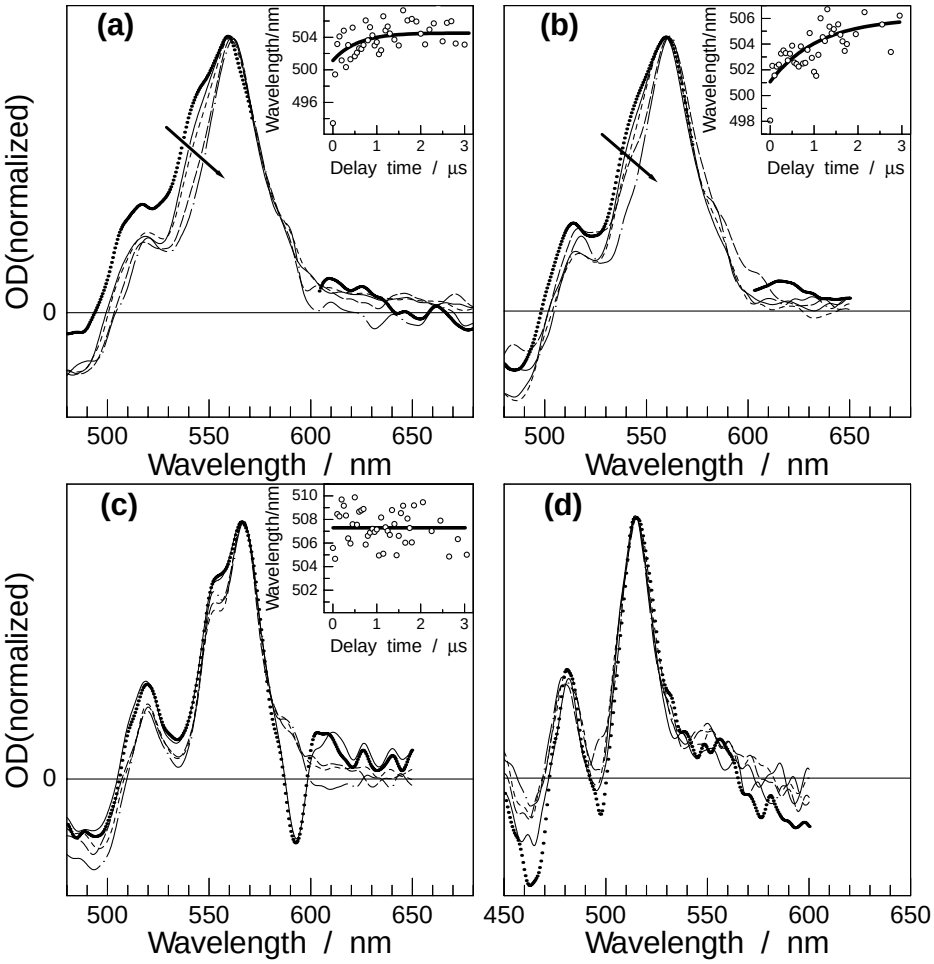

Figure 3. Normalized and smoothed 5 $T_n \leftarrow T_1$ transient absorption spectra between 0.00 and 2.00 μs, arrows in (a) and (b) indicate the sequence of delay time in the order of 0.00 → 0.05 → 0.30 → 1.00 → ~2.00 μs. Figures (a)–(d) correspond to those in Figure 2. Insets in (a)–(c) show the kinetics of the shift of isosbestic wavelength (open circles) together with fitting curves (thicker solid lines).

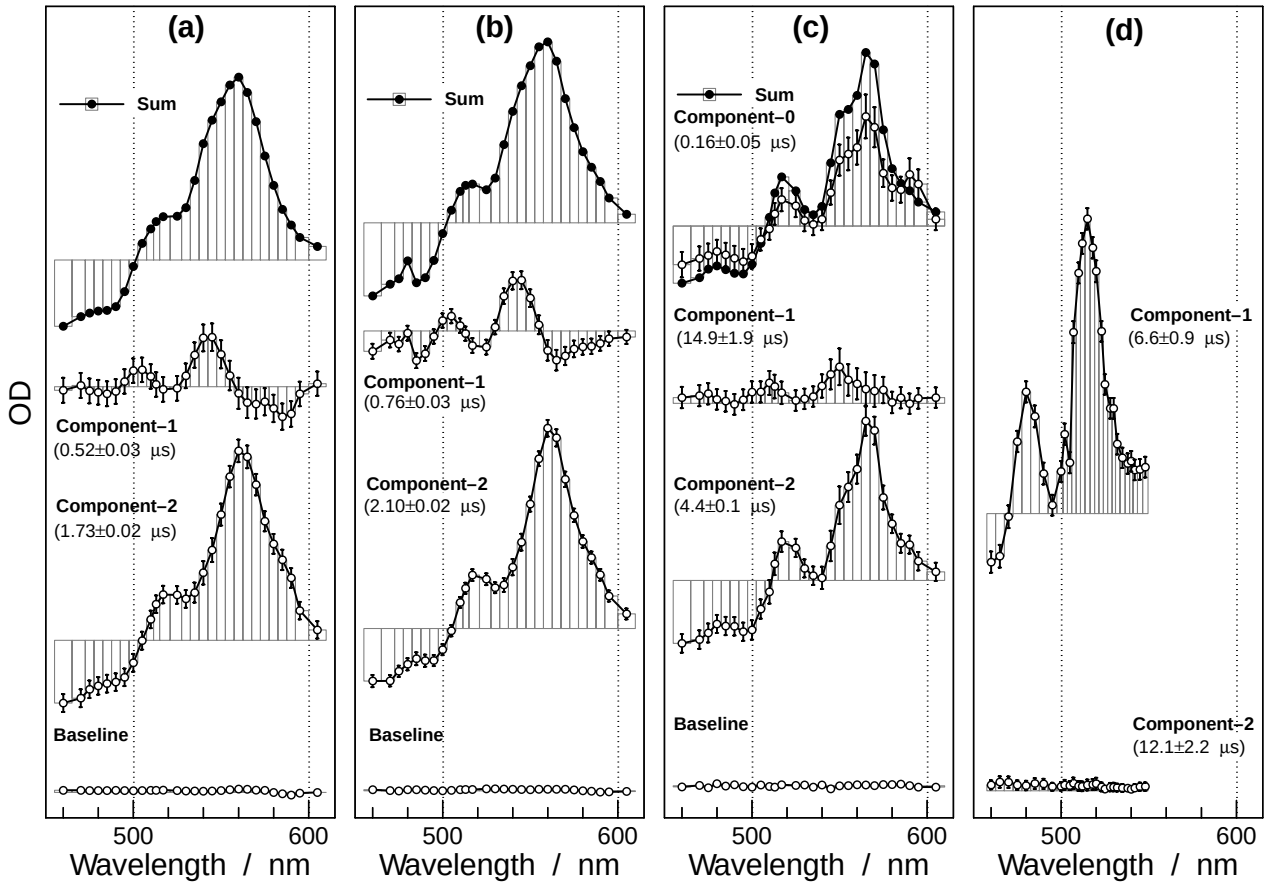

Figure 4. DADS components and associated time constants (in parentheses) derived from the global analysis on the sets of time-resolved spectra as shown in Figure 2 (see text for details). Figures (a)–(d) correspond to those in Figure 2. In panel (c) the rising component-0 is inverted for better comparison with the Sum spectrum.

decay-to-rise correlation between component-1 and component-2, the latter of which is also peaked at ~560 nm. This correlation suggests a transformation of excited population from component-1 to component-2 with the time constants of 0.52 ± 0.03 μs, and 0.76 ± 0.03 μs under aerobic (Figure 4a) and anaerobic (Figure 4b) condition, respectively. These timescales are in rough agreement with those of spectral equilibration derived directly from the kinetics of isosbestic wavelengths (0.6 and 1.1 μs). The negative feature at 585 nm, which is rather weak in the anaerobic case, may originate from triplet (monomethylated) spirilloxanthin because the $T_n \leftarrow T_1$ transition of spirilloxanthin locates at ~585 nm at room temperature (Monger et al. 1976; Kingma et al. 1985). The subsequent decay of triplet (monomethylated) spirilloxanthin appears as a weak shoulder that is distinguishable in the longer-wavelength side of component-2 in the aerobic case (Figure 4a). This particular spectral component could not be extracted independently owing to its low signal level in the original data sets (Figures 2a, b).

Component-2 in Figures 4a and b makes a major contribution to the Sum spectra. Its peak wavelength of 560 nm is a few nanometers shorter than the reported values of $T_n \leftarrow T_1$ transition for Cars having 12 conjugated double bonds in the LH2 complexes at low temperature (Angerhofer et al. 1995). Therefore, we attribute component-2 to the group of Cars having 12 conjugated bonds which occupies 38.6% of the overall Car content (Table 1).

At 77 K the DADS of the exponential increase component (component-0) is quite similar in key features as the Sum spectrum (Figure 4c), suggesting that components 1 to 2 all experienced a rising phase with the time constant of 0.16 ± 0.05 μs immediately following the pulsed excita-

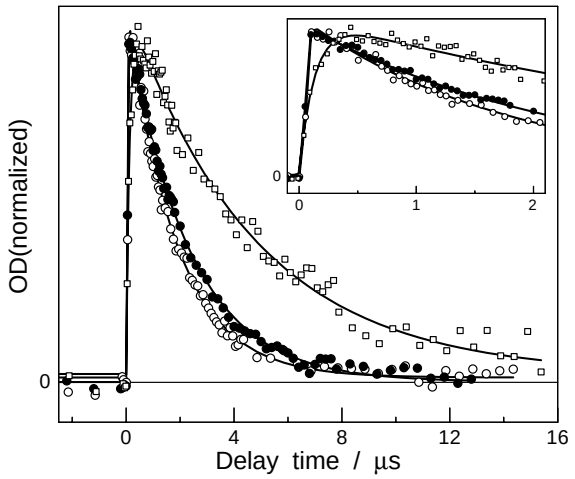

Figure 5. Kinetics traces plotted from the sets of time-resolved spectra as shown in Figure 2 at 560 nm for aerobic (open circles) and anaerobic (filled circles) cases under room temperature, and that plotted at 566 nm for the 77-K case (open squares). Solid lines are fitting curves obtained from the global curve-fitting procedures (see text for details). Inset shows the details of the initial delay-time range.

tion. Here again, component-1 that peaks at 550 nm can be ascribed to the group of Cars having 11 conjugated double bonds (lycopene and rhodopin), and components-2 at ~566 nm to those Cars having 12 (anhydrorhodovibrin, 3,4-didehydrorhodopin and rhodovibrin). The peak wavelengths of the $T_n \leftarrow T_1$ absorption of these two spectral components are both red shifted by ~5 nm with respect to the corresponding room-temperature values. In the DADS of component-0 a feature at ~590 nm can be clearly identified, which is most likely due to the interference from the excitation laser pulses as seen in the original data set (Figure 4c). Similar as the room-temperature case, the DADS of (monomethylated) spirilloxanthin was not unambiguously detected, and appeared only as a weak shoulder to the longer-wavelength side of the main absorption of component-2. In component-1 the negative spectral features seen at room temperature are not seen in the red edge of the main absorption band at 550 nm. Most importantly, the triplet excited-state lifetimes of component-1 and component-2, 14.9 ± 1.9 and 4.4 ± 0.1 μs, respectively, both prolonged significantly with reference to those in the room-temperature cases (0.5–0.8 and 1.7–2.1 μs), and the time constant of component-1 is considerably larger than that of component-2, which is opposite to the case of room temperature. The above results suggest that triplet excitation transfer from a shorter- to a longer-conjugated Car is essentially inactive at 77 K.

For the LH2 complex from *Rb. sphaeroides* G1C (Figure 4d), global analysis yielded 1 major DADS component with a decay time constant of 6.6 ± 0.9 μs (component-1), while component-2 is both weak and featureless, which can be regarded as a background. This result delivers an important piece of information that no appreciable spectral equilibration was observed for this LH2 complex that mainly contains a single type of Car.

Discussion

The present work has provided the first spectroscopic evidence on the equilibration dynamics of triplet excitation among different types of Cars in a bacterial antenna complex. We now discuss the structural information concerned with different types of Cars in an α,β-subunit based on our spectroscopic data.

At room temperature, rapid spectral relaxation was observed with a characteristic time constant of 0.6–1.1 μs as derived from the dynamic shift of isosbestic wavelengths around 500 nm (Figures 3a, b). This timescale is in rough agreement with the decay time constant of the shorter-conjugated Cars, 0.5–0.8 μs, obtained with the help of global spectral analysis (Figures 4a, b). Further, the dynamic relaxation observed in the ML–LH2 complex from *Rps. palustris* was not seen in the LH2 complex from *Rb. sphaeroides* G1C containing mainly a single type of Car. These together with the decay-to-rise correlation found between components 1 and 2 in Figures 4a and b lead us to ascribe the unique spectral relaxation to the reaction of triplet excitation transfer between different types of Cars, i.e., for energetic reasons, from lycopene/rhodopin to anhydrorhodovibrin/3,4-didehydrorhodopin/rhodovibrin, or likely to (monomethylated) spirilloxanthin. A structural prerequisite for the reaction to take place is the coexistence and the close proximity of the Car molecules in an α,β-subunit.

In the first 2.5-Å crystallographic structure of the LH2 from *Rps. acidophila*, the existence of a second Car molecule in an α,β-subunit was

ambiguous (McDermott et al. 1995; Freer et al. 1996). A later spectroscopic study suggested two Car molecules (Herek et al. 1998), whereas a careful stoichiometry study found only one (Arellano et al. 1998). Most recently, a 2.0-Å structure of the LH2 from *Rps. acidophila* was reported (Papiz et al. 2003), in which a second rhodopin glucoside molecule likely in a 12,15-*cis* configuration was found to keep van der Waals contact with both α- and β-B850s. For the LH2 complex from *Rs. molischianum* whose X-ray structure shows only one Car molecule in an α,β-subunit, there was a discussion on how this Car having close contact only with α-B850 can protect β-B850 and B800 (Damjanovic et al. 1999). The newly reported 2.0-Å data on *Rps. acidophila* would be helpful in clarifying this issue. For the ML–LH2 complex from *Rps. palustris*, our spectroscopic results suggest that Car molecules of $N_{C=C} = 11$ and 12 (13) coexist in an individual α,β-subunit. In fact, a recent time-resolved electron paramagnetic resonance (EPR) study on the LH2 complexes from a number of strains had shown clear polarization inversion in the spin-polarized triplet states of Cars, which could also be explained by assuming the Car-to-Car triplet exchange reaction although the authors rejected this possibility based on the believe that only one Car molecule exists in an α,β-subunit (Bittl et al. 2001).

In the set of original time-resolved absorption spectra at 77 K (Figure 2c), it seems that the 550 nm absorptive band decays even slower than the 566-nm band. This is in agreement with the results of global analysis that shorter-conjugated Cars ($N_{C=C} = 11$) live longer than longer-conjugated ones ($N_{C=C} = 12$). In addition, no apparent decay-to-rise correlation among the DADS components 1 to 2 can be recognized (Figure 4c). This situation is opposite to the room-temperature cases. For kinetics reasons we conclude that the excitation transfer from a shorter- to a longer-conjugated Car is less efficient at 77 K than at room temperature. Therefore the reaction of Car-to-Car triplet excitation transfer is temperature dependent. Since the triplet excitation energy of a shorter-conjugated Car is higher than that of a longer-conjugated one (Farhoosh et al. 1994), it is reasonable that the Car-to-Car energy transfer process is energetically feasible both at room temperature and at 77 K. The temperature-dependent behavior may originate from the spectral narrowing of the phosphorescence spectrum of the donor Car and the effective $T_1 \leftarrow S_0$ absorption spectrum of the acceptor Car upon decreasing temperature, which would result in a smaller spectral integral in the formulism of transition probability by the exchange mechanism (Dexter 1953).

The initial building-up phase of $T_n \leftarrow T_1$ absorption, which reflects the process of BChl-to-Car energy transfer, was clearly observed at 77 K (Figure 2c, 5) although not seen at room temperature owing to the limited instrumental resolution (Figures 2a, b). As revealed by the use of global analysis for the 77-K data (Figure 4c), the DADS of component-0, which consists of the contribution from all the two groups of Cars and increases with a time constant of 0.16 ± 0.05 μs, is almost identical in spectral patterns to the Sum spectrum obtained by adding up the subsequent components. This suggests that ^{3}BChl* transfers triplet excitation to different groups of Cars with the number of conjugated bonds from 11 to 13. Here again, all the three groups of Cars must keep van der Waals contact with BChl molecules in the antenna complexes for efficient BChl-to-Car triplet energy transfer to take place.

In summary, the present study has shown that Cars of 11 conjugated bonds transfer their triplet energy to those of 12 or 13 conjugated bonds, and that BChl molecules transfer their triplet excitation to Cars with the number of conjugated bonds from 11 to 13 in the ML–LH2 complex from *Rps. palustris*. These reactions of triplet excitation transfer exhibit temperature dependence. Based on the above results and those of the pigment composition analysis, we propose that Cars of 11 and 12 13) conjugated bonds, both in close proximity of BChls, may coexist in an α,β-subunit of the ML–LH2 complex.

Acknowledgements

This work has been supported by grants from the Natural Science Foundation of China (#20273077; #39890390), and the State Key Basic Research and Development Plan (#G1998010100). JPZ is indebted to a support from the Hundred-Talent Project of CAS.

References

Allen JP, Feher G, Yeates TO, Komiya H and Rees DC (1987) Structure of the reaction centre from *Rhodobacter sphaeroides* R-26: the cofactors. Proc Natl Acad Sci USA 84: 5730–5734

Angerhofer A, Bornhäuser F, Gall A and Cogdell RJ (1995) Optical and optically detected magnetic resonance investigation on purple photosynthetic bacterial antenna complexes. Chem Phys 194: 259–274

Arellano JB, Raju BB, Naqvi KR and Gillbro T (1998) Estimation of pigment stoichiometries in photosynthetic systems of purple bacteria: special reference to the (absence of) second carotenoid in LH2. Photochem Photobiol 68: 84–87

Bittl R, Schlodder E, Geisenheimer I, Lubitz W and Cogdell RJ (2001) Transient EPR and absorption studies of carotenoid triplet formation in purple bacterial antenna complexes. J Phys Chem B 105: 5525–5535

Bose SK (1963) Media for anaerobic growth of photosynthetic bacteria. In: Gest H, Pietro AS and Vernon LP (eds) Bacterial Photosynthesis, pp 501–511. The Antioch Press, Yellow Springs, Ohio

Clayton RK (1966) Spectroscopic analysis of bacteriochlorophylls *in vitro* and *in vivo*. Photochem Photobiol 5: 669–677

Cogdell RJ, Hipkins MF, MacDonald W and Truscott TG (1981) Energy transfer between the carotenoid and the bacteriochlorophyll within the B-800–850 light-harvesting pigment-protein complex of *Rhodopseudomonas sphaeroides*. Biochim Biophys Acta 634: 191–202

Cogdell RJ, Howard TD, Bittl R, Schlodder E, Geisenheimer I and Lubitz W (2000) How carotenoids protect bacterial photosynthesis. Phil Trans R Soc London Ser B 355: 1345–1349

Connolly JS, Samuel EB and Janzen F (1982) Effects of solvent on the fluorescence properties of bacteriachlorophyll a. Photochem Photobiol 36: 565–574

Crystall B, Booth PJ, Klug DR, Barber J and Porter G (1989) Resolution of a long lived fluorescence component from D1/D2/cytochrome *b*-559 reaction centres. FEBS Lett 249: 75–78

Deisenhofer J, Epp O, Miki K, Huber R and Michel H (1985) Structure of the protein subunits in the photosynthetic reaction center of *Rhodopseudomonas viridis* at 3 Å resolution. Nature 318: 618–624

Damjanović A, Ritz T and Schulten K (1999) Energy transfer between carotenoids and bacteriochlorophylls in light-harvesting complex II of purple bacteria. Phys Rev E 59: 3293–3311

Dexter DL (1953) A theory of sensitized luminescence in solids. J Chem Phys 21: 836–850

Ermler U, Fritzsch G, Buchanan SK and Michel H (1994) Structure of the photosynthetic reaction centre from *Rhodobacter sphaeroides* at 2.65 Å resolution: cofactors and protein-cofactor interactions. Structure 2: 925–936

Evans MB, Hawthornthwaite AM and Cogdell RJ (1990) Isolation and characterization of the different B800–B850 light-harvesting complexes from low- and high-light grown cells of *Rhodopseudomonas palustris*, strain 2.1.6. Biochim Biophys Acta. 1016: 71–76

Farhoosh R, Chynwat V, Gebhard R, Lugtenburg J and Frank HA (1994) Triplet energy transfer between bacteriochlorophyll and carotenoids in B850 light–harvesting complexes of *Rhodobacter sphaeroides* R-26.1. Photosynth Res 42: 157–166

Frank HA and Cogdell RJ (1993) The photochemistry and function of carotenoids in photosynthesis. In: Young A and Britton G (eds) Carotenoids in Photosynthesis, pp 252–321. Chapman & Hall, London

Freer A, Prince S, Sauer K, Papiz M, Hawthornthwaite-Lawless A, McDermott G, Cogdell R and Isaacs NW (1996) Pigment-pigment interactions and energy transfer in the antenna complex of the photosynthetic bacterium *Rhodopseudomonas acidophila*. Structure 4: 449–462

Fujii R, Onaka K, Kuki M, Koyama Y and Watanabe Y (1998) The $2A_g^-$ energies of all-*trans*-neurosporene and spheroidene as determined by fluorescence spectroscopy. Chem Phys Lett 288: 847–853

Gradinaru CC, Kennis JTM, Papagiannakis E, van Stokkum IHM, Cogdell RJ, Fleming GR, Niederman RA and van Grondelle R (2001) An unusual pathway of excitation energy deactivation in carotenoids: singlet-to-triplet conversion on an ultrafast timescale in a photosynthetic antenna. Proc Natl Acad Sci USA 98: 2364–2369

Hartigan N, Tharia HA, Sweeney F, Lawless AM and Papiz MZ (2002) The 7.5-Å electron density and spectroscopic properties of a novel low-light B800 LH2 from *Rhodopseudomonas palustris*. Biophys J 82: 963–977

Herek JL, Polívka T, Pullerits T, Fowler GJS, Hunter CN and Sundström V (1998) Ultrafast carotenoid band shifts probe structure and dynamics in photosynthetic antenna complexes. Biochemistry 37: 7057–7061

Kingma H, van Grondelle R and Duysens LNM (1985) Magnetic-field effects in photosynthetic bacteria. II. Formation of triplet states in the reaction center and the antenna of *Rhodospirillum rubrum* and *Rhodopseudomonas sphaeroides*. Magnetic-field effects. Biochim Biophys Acta 808: 383–399

Koepke J, Hu X, Muenke C, Schulten K and Michel H (1996) The crystal structure of the light-harvesting complex II (B800–B850) from *Rhodospirillum molischianum*. Structure 4: 581–597

Koyama Y, Kuki M, Andersson PO and Gillbro T (1996) Singlet excited states and the light harvesting function of carotenoids in bacterial photosynthesis. Photochem Photobiol 63: 243–256

McDermott G, Prince SM, Freer AA, Hawthornthwaite-Lawless AM, Papiz MZ, Cogdell RJ and Isaacs NW (1995) Crystal Structure of an integral membrane light-harvesting complex from photosynthetic bacteria. Nature 374: 517–521

Monger TG, Cogdell RJ and Parson WW (1976) Triplet states of bacteriochlorophyll and carotenoids in chromatophores of photosynthetic bacteria. Biochim Biophys Acta 449: 136–153

Monger TG and Parson WW (1977) Singlet-triplet fusion in *Rhodopseudomonas sphaeroides* chromatophores, a probe of the organization of the photosynthetic apparatus. Biochim Biophys Acta 460: 393–407

Nagae H, Kakitani T, Katoh T and Mimuro M (1993) Calculation of the excitation transfer-matrix elements between the S_2 or S_1 state of carotenoid and the S_2 or S_1 state of bacteriochlorophyll. J Chem Phys 98: 8012–8023

Papiz MZ, Prince SM, Howard T, Cogdell RJ and Isaacs NW (2003) The structure and thermal motion of the B800–850 LH2 complex from *Rps. acidophila* at 2.0 Å resolution and

100 K: new structural features and functionally relevant motions. J Mol Biol 326: 1523–1538

Qian P, Saiki K, Mizoguchi T, Hara K, Sashima T, Fujii R and Koyama Y (2001) Time-dependent changes in the carotenoid composition and preferential binding of spirilloxanthin to the reaction center and anhydrorhodovibrin to the LH1 antenna complex in *Rhodobium marinum*. Photochem Photobiol 74: 444–452

Rademaker H, Hoff AJ, van Grondelle R and Duysens LNM (1980) Carotenoid triplet yields in normal and deuterated *Rhodospirillum Rubrum*. Biochim Biophys Acta 592: 240–257

Ritz T, Damjanovic A, Schulten K, Zhang JP and Koyama Y (2000) Understanding efficient light-harvesting through carotenoids with novel theoretical and experimental techniques, Photosynth Res 66: 125–144

Schmidt K (1978) Biosynthesis of carotenoids. In: Clayton RK and Sistrom WR (eds) The Photosynthetic Bacteria, pp 729–750. Plenum Press, New York

Tharia HA, Nightingale TD, Papiz MZ and Lawless AM (1999) Characterization of hydrophobic peptides by RP-HPLC from different spectral forms of LH2 isolated from *Rps. palustris*. Photosynth Res 61: 157–167

Truscott TG, Land EJ and Sykes A (1973) The *in vitro* photochemistry of biological molecules-III. Absorption spectra, lifetimes and rates of oxygen quenching of the triplet states of β-carotene, retinal and related polyenes. Photochem Photobiol 17: 43–51